Coulomb force effects in low-energy α-deuteron scattering

A. Deltuva*
Centro de Física Nuclear da Universidade de Lisboa, P-1649-003 Lisboa, Portugal
(Received 10 October 2006; published 6 December 2006)

The α-proton Coulomb interaction is included in the description of α-deuteron scattering using the screening and renormalization approach in the framework of momentum-space three-particle equations. The technical reliability of the method is demonstrated. Large Coulomb-force effects are found.

DOI: 10.1103/PhysRevC.74.064001 PACS number(s): 21.45.+v, 21.30.−x, 24.70.+s, 25.10.+s

I. INTRODUCTION

The application of exact Faddeev three-body theory to the understanding of nuclear reactions that are dominated, at low energies, by three-body degrees of freedom has been shadowed in the past by the difficulty in dealing with the long-range Coulomb interaction between charged particles. Up to now this difficulty has been overcome by the use of approximate theoretical methods, namely, the continuum-discretized coupled-channel (CDCC) method [1], which was proposed initially to deal with deuteron scattering on a heavier nuclei, but that is now widely used to analyze data resulting from the reactions involving halo nuclei. Given the progress achieved recently in the description of proton-deuteron (pd) elastic scattering and breakup using exact three-body equations [2–4], we are now able to include the Coulomb interaction in three-body nuclear reactions involving two charged particles. Before we apply the present method to the description of direct nuclear reactions that are dominated by three-body degrees of freedom, we show here the results for alpha-deuteron (αd) scattering which at low energies is one of simplest effective three-body nuclear reactions.

The αd scattering has been studied extensively in the past, both experimentally and theoretically [5–12]. Although αd is a six-nucleon system, at low energies, to a good approximation, the α particle may be considered a spin zero structureless boson, and thereby the theoretical description of αd scattering may be reduced to a three-body problem made up of one α and two nucleons (N). Then, the most serious difficulty is the treatment of the long-range Coulomb interaction, which in the previous calculations was either completely neglected or taken into account only approximately. Using the method developed in Refs. [2–4] we are now able to include the Coulomb interaction also for αd scattering, quantitatively evaluate its importance, and with greater confidence ascertain the quality of αN force models.

Section II shortly recalls the technical apparatus underlying the calculations. Section III presents characteristic results. Section IV gives our conclusions.

*Electronic address: deltuva@cii.fc.ul.pt

II. TREATMENT OF THE COULOMB INTERACTION USING THE SCREENING AND RENORMALIZATION APPROACH

Our treatment of the Coulomb interaction is based on the idea of screening and renormalization proposed in Ref. [13] for two-particle scattering and extended in Refs. [2,3,14,15] to three-particle scattering where only two particles are charged. The Coulomb potential is screened, standard scattering theory is applicable, and the renormalization procedure is applied to recover the unscreened limit. The success of the method depends on the choice of the screened Coulomb potential

$$w_R(r) = w(r)\, e^{-(r/R)^n}. \tag{1}$$

We prefer to work with a sharper screening than the Yukawa screening ($n = 1$) of Ref. [15]. We want to ensure that the screened Coulomb potential $w_R(r)$ approximates well the true Coulomb one $w(r)$ for distances r smaller than the screening radius R and simultaneously vanishes rapidly for $r > R$, providing a comparatively fast convergence of the partial-wave expansion. In contrast, the sharp cutoff ($n \to \infty$) yields an unpleasant oscillatory behavior in the momentum-space representation, leading to convergence problems. In Refs. [2,3] we found the values $3 \leqslant n \leqslant 6$ to provide a sufficiently smooth, but at the same time a sufficiently rapid screening around $r = R$; $n = 4$ is our choice also in the present paper.

We solve Alt-Grassberger-Sandhas (AGS) three-particle scattering equations [16] in momentum space

$$U^{(R)}_{\beta\alpha}(Z) = \bar{\delta}_{\beta\alpha} G_0^{-1}(Z) + \sum_\sigma \bar{\delta}_{\beta\sigma} T^{(R)}_\sigma(Z) G_0(Z) U^{(R)}_{\sigma\alpha}(Z), \tag{2a}$$

$$U^{(R)}_{0\alpha}(Z) = G_0^{-1}(Z) + \sum_\sigma T^{(R)}_\sigma(Z) G_0(Z) U^{(R)}_{\sigma\alpha}(Z), \tag{2b}$$

with $\bar{\delta}_{\beta\alpha} = 1 - \delta_{\beta\alpha}$, $G_0(Z)$ being the free resolvent, $T^{(R)}_\sigma(Z)$ the two-particle transition matrix derived from nuclear plus screened Coulomb potentials, and $U^{(R)}_{\beta\alpha}(Z)$ and $U^{(R)}_{0\alpha}(Z)$ the three-particle transition operators for elastic/rearrangement and breakup scattering; their dependence on the screening radius R is notationally indicated. On-shell matrix elements of the operators (2) between two- and- three-body channel states $|\phi_\alpha(\mathbf{q}_i)\nu_{\alpha_i}\rangle$ and $|\phi_0(\mathbf{p}_f \mathbf{q}_f)\nu_{0_f}\rangle$ with discrete quantum numbers ν_{σ_j}, Jacobi momenta $\mathbf{p}_j$ and $\mathbf{q}_j$, energy E_i, and $Z = E_i + i0$, do not have a $R \to \infty$ limit. However, as demonstrated in Refs. [2,3,14], the three-particle amplitudes can be decomposed into long-range and Coulomb-distorted short-range

parts, where the quantities diverging in that limit are of two-body nature, i.e., the on-shell transition matrix $T^{\rm c.m.}_{\alpha R}(Z)$ derived from the screened Coulomb potential between spectator and the center of mass (c.m.) of the bound pair, the corresponding wave function, and the screened Coulomb wave function for the relative motion of two charged particles in the final state. Those quantities, renormalized according to Ref. [13], in the $R \to \infty$ limit converge to the two-body Coulomb scattering amplitude $\langle \phi_\alpha(\mathbf{q}_f)\nu_{\alpha_f}|T^{\rm c.m.}_{\alpha C}|\phi_\alpha(\mathbf{q}_i)\nu_{\alpha_i}\rangle$ (in general, as a distribution) and to the corresponding Coulomb wave functions, respectively, thereby yielding the three-particle scattering amplitudes in the proper Coulomb limit

$$\begin{aligned}
&\langle \phi_\beta(\mathbf{q}_f)\nu_{\beta_f}|U_{\beta\alpha}|\phi_\alpha(\mathbf{q}_i)\nu_{\alpha_i}\rangle \\
&\quad = \delta_{\beta\alpha}\langle \phi_\alpha(\mathbf{q}_f)\nu_{\alpha_f}|T^{\rm c.m.}_{\alpha C}|\phi_\alpha(\mathbf{q}_i)\nu_{\alpha_i}\rangle \\
&\qquad + \lim_{R\to\infty}\Big\{\mathcal{Z}^{-\frac{1}{2}}_{\beta R}(q_f)\langle \phi_\beta(\mathbf{q}_f)\nu_{\beta_f}|\Big[U^{(R)}_{\beta\alpha}(E_i+i0) \\
&\qquad - \delta_{\beta\alpha}T^{\rm c.m.}_{\alpha R}(E_i+i0)\Big]|\phi_\alpha(\mathbf{q}_i)\nu_{\alpha_i}\rangle \mathcal{Z}^{-\frac{1}{2}}_{\alpha R}(q_i)\Big\}, \qquad (3a)
\end{aligned}$$

$$\begin{aligned}
&\langle \phi_0(\mathbf{p}_f\mathbf{q}_f)\nu_{0_f}|U_{0\alpha}|\phi_\alpha(\mathbf{q}_i)\nu_{\alpha_i}\rangle \\
&\quad = \lim_{R\to\infty}\Big\{z^{-\frac{1}{2}}_R(p_f)\langle \phi_0(\mathbf{p}_f\mathbf{q}_f)\nu_{0_f}| \\
&\qquad \times U^{(R)}_{0\alpha}(E_i+i0)|\phi_\alpha(\mathbf{q}_i)\nu_{\alpha_i}\rangle \mathcal{Z}^{-\frac{1}{2}}_{\alpha R}(q_i)\Big\}. \qquad (3b)
\end{aligned}$$

The renormalization factors $\mathcal{Z}_{\alpha R}(q_j)$ and $z_R(p_f)$ are diverging phase factors given in Refs. [2,3,13,14]. The $R \to \infty$ limit in Eqs. (3) has to be calculated numerically, but due to the short-range nature of the corresponding operators it is reached with sufficient accuracy at rather modest R if the form of the screened Coulomb potential has been chosen successfully as discussed above. More details on the practical implementation of the screening and renormalization approach are given in Refs. [2–4]. Compared to the pd calculations an additional difficulty is the presence of the αN P-wave transition matrix $T^{(R)}_\sigma(Z)$ poles in the complex energy plane close to the real axis. This requires special treatment of those partial waves in the numerical solution of Eqs. (2), i.e., the pole factor of $T^{(R)}_\sigma(Z)$ is separated when interpolating $T^{(R)}_\sigma(Z)G_0(Z)U^{(R)}_{\sigma\alpha}(Z)$ and the subtraction technique is used for integration.

III. RESULTS

There exist in the literature several parametrizations of the αN potential. Most of them support deeply bound αN state in S-wave that is not observed experimentally, since it is forbidden by the Pauli principle. To account for the Pauli principle that forbidden state $|b\rangle$ (or some state close to it) has to be projected out or moved to a large positive energy Γ, replacing the potential v by $v' = v + |b\rangle\Gamma\langle b|$. As demonstrated in Ref. [17], the latter method in the $\Gamma \to \infty$ limit is equivalent to the first one. Alternatively, one may use repulsive αN potential in the S-wave. In order to estimate the model dependence, in the calculations of this paper we use three different parametrizations for the nuclear part of the αN potential, that in the following will be called αN-I, αN-II, and αN-III. The potential αN-I is taken from Ref. [18]. It is of Woods-Saxon form with central and spin-orbit parts and supports a bound-state in S-wave that is moved to a large positive energy Γ; we found that for $\Gamma \geqslant 1000$ MeV the results are practically independent of Γ. The potential αN-II is taken from Ref. [18] as well and differs from αN-I only in S-wave where it is repulsive and local, but, nevertheless, nearly phase equivalent to αN-I. The third potential αN-III, taken from Ref. [10], is represented as a sum of Gaussians with the strong repulsive rank-1 separable term in S-wave that moves the harmonic oscillator ground state which is close to the Pauli-forbidden state to $\Gamma = 1000$ MeV. The potentials fit the low energy experimental αN phase shifts quite well, although αN-III is more attractive in P-waves than the other two. All potentials are charge symmetric and act in partial waves with orbital angular momentum $L \leqslant 2$. For the neutron-proton (np) interaction we use the charge dependent (CD) Bonn potential [19] and include partial waves with total angular momentum $I \leqslant 2$ plus $^3D_3$. It was checked that those quite low partial waves are sufficient for convergence. In contrast, the screened Coulomb potential is of longer range and therefore, depending on the screening radius R, requires partial waves up to $L \leqslant 11$. Those high partial waves are included exactly as described in Ref. [4]. We note that the αp Coulomb potential at short distances is taken as the one of a uniformly charged sphere, i.e., $w(r) = 2\alpha_e[3 - (r/R_I)^2]/(2R_I)$ for $r < R_I = 1.5$ fm, α_e being the fine structure constant.

The internal criterion for the reliability of the screening and renormalization approach is the convergence of the observables with the screening radius R employed to calculate the Coulomb-distorted short-range part of the amplitudes in Eq. (3); that criterion was found to be absolutely reliable for pd scattering [20]. Figures 1 and 2 show several examples for αd elastic scattering and breakup. The breakup kinematical final-state configurations are characterized in a standard way by the polar angles of the α-particle and the proton and by the azimuthal angle between them, $(\theta_\alpha, \theta_p, \varphi_p - \varphi_\alpha)$. The definition of the arclength S along the kinematical curve is the standard one as in Refs. [8–10]. Even when the Coulomb effect is large the convergence is impressively fast, e.g., the screening radius $R = 10$ fm is practically sufficient for the elastic αd scattering at 4.81 MeV deuteron laboratory energy in Fig. 1, while the observables of αd breakup at 15 MeV α laboratory energy in Fig. 2 require at least $R = 15$ fm for convergence. As discussed in Refs. [2,3], the convergence rate is energy dependent, i.e., larger screening radii are needed for elastic scattering observables at very low energies and for the breakup differential cross section in kinematical situations characterized by very low relative energy of the two charged particles, i.e., close to the αp final-state interaction (FSI) regime. Nevertheless, the observed convergence strongly suggests the reliability of the present Coulomb treatment using screening and renormalization approach.

As already shown in Figs. 1 and 2 the Coulomb effect on the observables of low energy αd scattering may be very strong, indicating that the inclusion of the Coulomb interaction is necessary for a stringent comparison of the theoretical results and experimental data. Obviously, we have many more

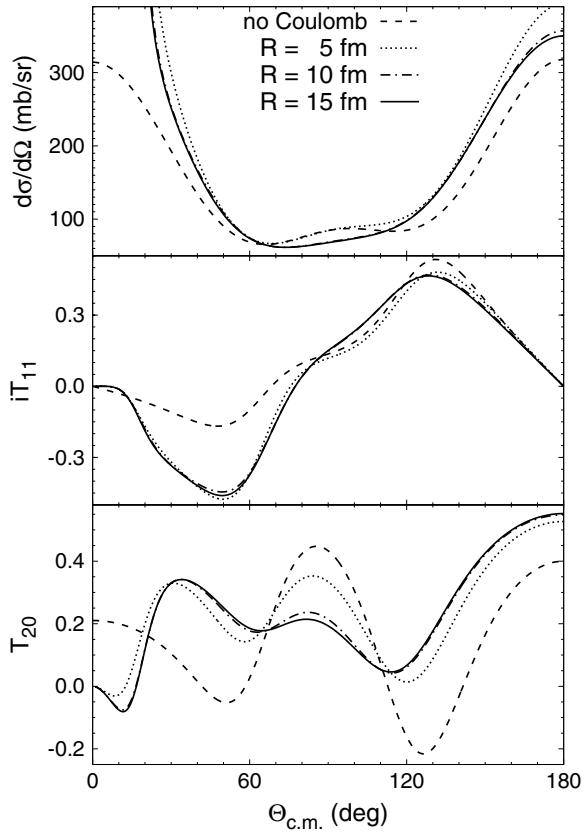

FIG. 1. Convergence of the αd elastic scattering observables with screening radius R. The differential cross section and deuteron analyzing powers iT_{11} and T_{20} at 4.81 MeV deuteron lab energy are shown as functions of the c.m. scattering angle. Results obtained with screening radius $R = 5$ fm (dotted curves), 10 fm (dash-dotted curves), and 15 fm (solid curves) are compared. Results without Coulomb (dashed curves) are given as reference for the size of the Coulomb effect. The calculations were performed with the αN-I potential.

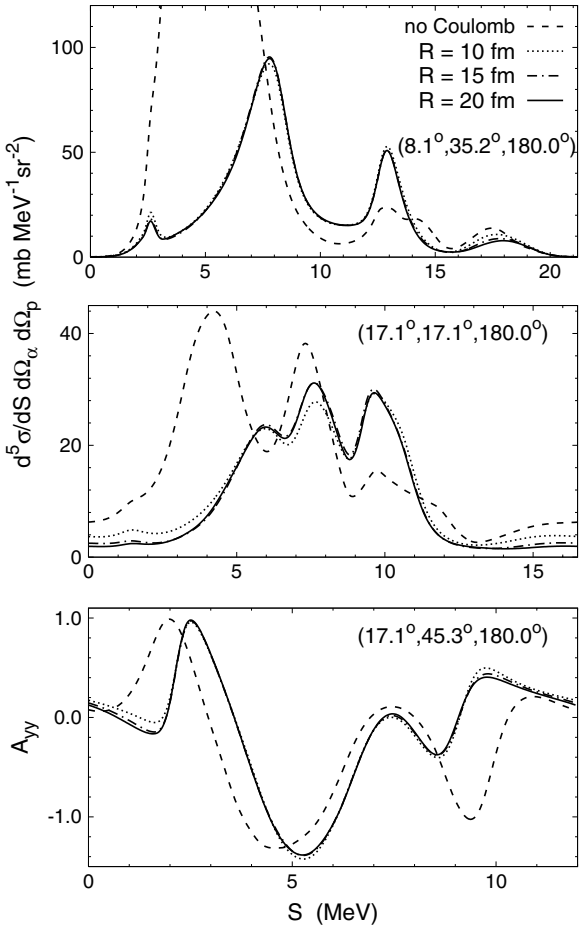

FIG. 2. Convergence of the αd breakup observables with screening radius R. The differential cross section and deuteron analyzing power A_{yy} in selected kinematical configurations at 15 MeV α lab energy are shown as functions of the arclength S along the kinematical curve. Results obtained with screening radius $R = 10$ fm (dotted curves), 15 fm (dash-dotted curves), and 20 fm (solid curves) are compared. Results without Coulomb (dashed curves) are given as reference for the size of the Coulomb effect. The calculations were performed with the αN-I potential.

predictions than it is possible to show. Therefore we make a selection of the most interesting predictions which illustrate the message we believe the results tell us. The readers are welcome to obtain the results for their favorite data from us.

Figure 3 presents our results for the differential cross section and all deuteron analyzing powers of elastic αd scattering at 4.81 MeV and 17 MeV deuteron laboratory energy. As expected, the Coulomb effect is large at lower energy for all observables in the whole angular regime, while with increasing energy it becomes smaller. Furthermore, the results depend strongly on the choice of the αN interaction. The potential αN-I describes most of the experimental $E_d = 4.81$ MeV data quite satisfactorily, whereas the potential αN-II that avoids the Pauli forbidden state in S-wave by the local repulsion clearly fails in accounting for the scattering data, especially at $E_d =$ 17 MeV, although the ^{6}Li bound state properties predicted by both potentials are very similar. The potential αN-III also fails in accounting for the experimental data at $E_d = 4.81$ MeV, but the difference between predictions using αN-I and αN-III is found to be mostly due to the differences in P-waves. At $E_d = 17$ MeV, which is just 3 MeV below ^{3}H + ^{3}He threshold, there is a qualitative agreement between experimental data and predictions with αN-I and αN-III, except for deuteron tensor analyzing powers T_{20} and T_{21}. Obviously, the treatment of the α-particle as a structureless boson becomes less reliable with increasing energy.

Figure 4 presents our results for the differential cross section of αd breakup at 15 MeV α laboratory energy in various kinematical configurations. The most important Coulomb effect is the shift of the αp P-wave resonance position that leads to the corresponding changes in the structure of the observables. Furthermore, the Coulomb interaction breaks $\alpha n - \alpha p$ charge symmetry and thereby allows the coupling to the np isospin triplet waves, in particular $^1S_0$. The predictions without Coulomb fail completely in accounting for the experimental data, while inclusion of the Coulomb moves the peaks of the differential cross section to the right positions, although the height of those peaks is not always reproduced. There is a strong dependence on the

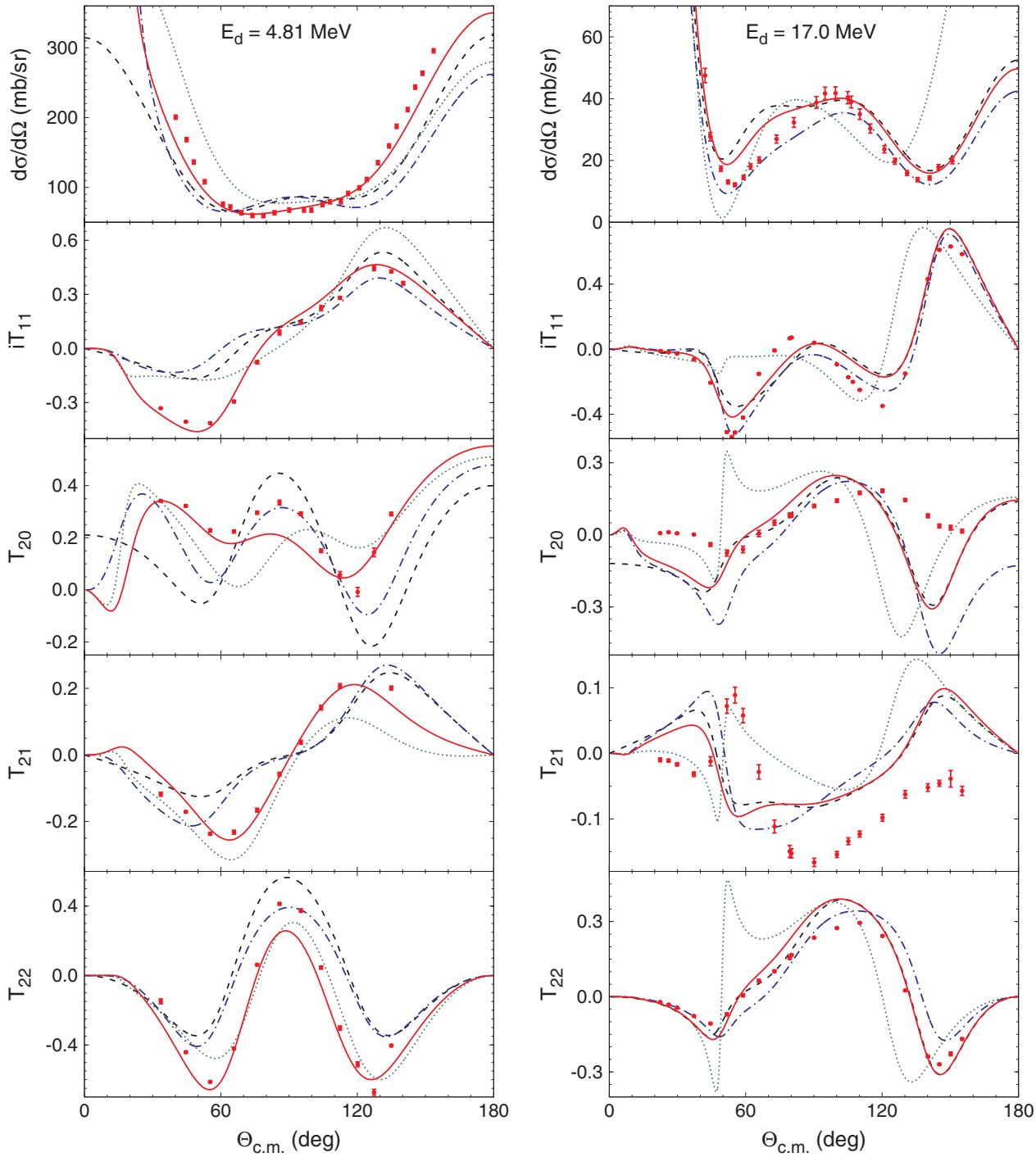

FIG. 3. (Color online) The differential cross section and deuteron analyzing powers at 4.81 MeV and 17 MeV deuteron lab energy. Results including the Coulomb interaction obtained with potentials αN-I (solid curves), αN-II (dotted curves), and αN-III (dash-dotted curves) are compared. αN-I results without Coulomb (dashed curves) are given as reference for the size of the Coulomb effect. The experimental 4.81-MeV data are from Ref. [7] for the differential cross section and from Ref. [5] for the spin observables, and the 17-MeV data are from Ref. [6].

employed αN potential, where, like in the elastic scattering, the potential αN-II provides the worst description of the data, and the difference between the predictions of αN-I and αN-III is dominated by the P-waves. The sensitivity of the results to the choice of a realistic np potential is also checked and found to be insignificant. When the c.m. energy increases one finds a larger part of the phase space where the relative αp energy may be quite different from the one corresponding to the P-wave resonance and therefore also the Coulomb effect is less significant as shown in Fig. 5.

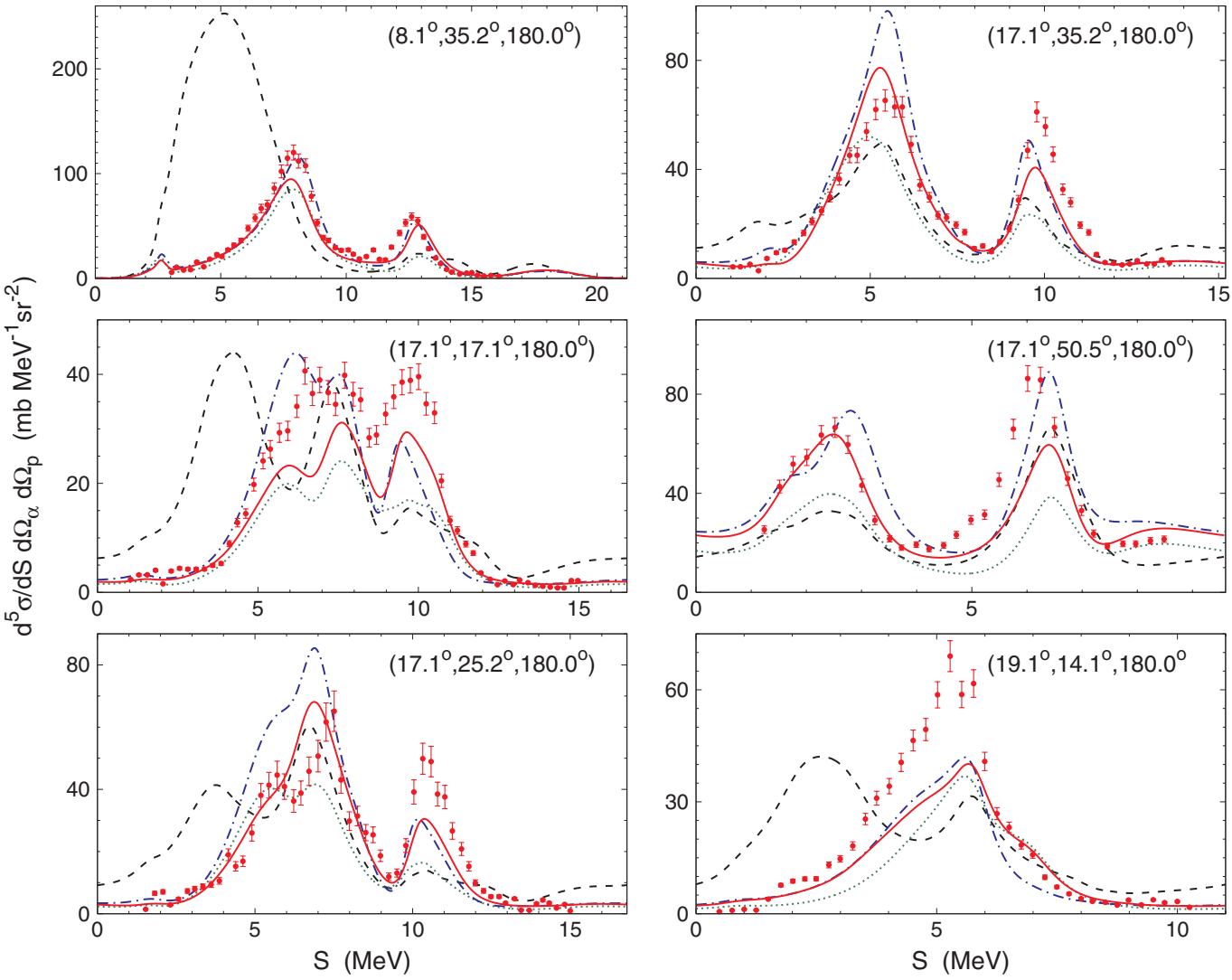

FIG. 4. (Color online) The differential cross section of the αd breakup at 15 MeV α lab energy in selected kinematical configurations. Curves as in Fig. 3. The experimental data are from Ref. [8].

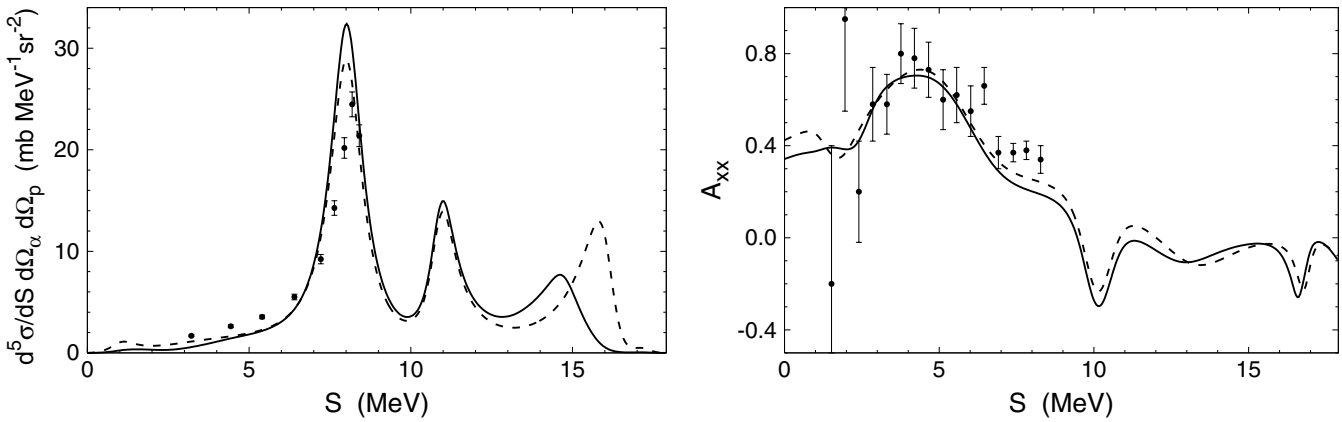

FIG. 5. The differential cross section and deuteron analyzing power A_{xx} of the αd breakup at 12 MeV deuteron lab energy in the (25°, 45°, 180°) configuration. Results obtained using the potential αN-I with (without) Coulomb are shown as solid (dashed) curves. The experimental data are from Ref. [9].

IV. SUMMARY

In this paper we show that the screening and renormalization approach for the inclusion of the Coulomb interaction in the description of three-particle scattering using momentum-space integral equations, developed in Refs. [2–4] for pd reactions, can be extended reliably to αd scattering. This is an important step towards application of exact scattering equations for the description of nuclear reactions within three-body models, where up to now only approximate treatments like the CDCC method [1] have been used.

The Coulomb effect on the observables of αd scattering is studied and is found to be large in elastic scattering at very low energies and in breakup, where the shift of αp P-wave resonance position leads to the corresponding shifts of the differential cross section peaks.

Another important consequence of this work is that it allows to ascertain with greater confidence the quality of the αN force models one uses to describe αd observables as well as structure and reactions of ^{6}Li and ^{6}He. Although at present there are too large uncertainties in the parametrization of P- and D-wave interactions that need to be improved, this work clearly indicates the superiority of the attractive S-wave potentials supporting a Pauli-forbidden state (that is projected out or moved to a large positive energy) over the repulsive S-wave potentials.

ACKNOWLEDGMENTS

The author thanks A. C. Fonseca for many discussions and suggestions, and W. Grüebler for providing experimental data. The work is supported by the Fundação para a Ciência e a Tecnologia (FCT) grant SFRH/BPD/14801/2003.

[1] N. Austern, Y. Iseri, M. Kamimura, M. Kawai, G. Rawitscher, and M. Yahiro, Phys. Rep. **154**, 125 (1987).
[2] A. Deltuva, A. C. Fonseca, and P. U. Sauer, Phys. Rev. C **71**, 054005 (2005).
[3] A. Deltuva, A. C. Fonseca, and P. U. Sauer, Phys. Rev. C **72**, 054004 (2005).
[4] A. Deltuva, A. C. Fonseca, and P. U. Sauer, Phys. Rev. C **73**, 057001 (2006).
[5] W. Grüebler, V. König, P. A. Schmelzbach, and P. Marmier, Nucl. Phys. **A134**, 686 (1969); **A148**, 380 (1970); **A148**, 391 (1970).
[6] W. Grüebler, R. E. Brown, F. D. Correll, R. A. Hardekopf, N. Jarmie, and G. G. Ohlsen, Nucl. Phys. **A331**, 61 (1979).
[7] M. Bruno, F. Cannata, M. D'Agostino, C. Maroni, and M. Lombardi, Lett. Nuovo Cimento **27**, 265 (1980).
[8] I. Koersner, L. Glantz, A. Johansson, B. Sundqvist, H. Nakamura, and H. Noya, Nucl. Phys. **A286**, 431 (1977).
[9] I. Slaus, J. M. Lambert, P. A. Treado, F. D. Correll, R. E. Brown, R. A. Hardekopf, N. Jarmie, Y. Koike, and W. Grüebler, Nucl. Phys. **A397**, 205 (1983).
[10] P. Niessen, S. Lemâitre, K. R. Nyga, G. Rauprich, R. Reckenfelderbäumer, L. Sydow, H. Paetz gen. Schieck, and P. Doleschall, Phys. Rev. C **45**, 2570 (1992).
[11] Y. Koike, Nucl. Phys. **A301**, 411 (1978); **A337**, 23 (1980).
[12] K. Hahn, E. W. Schmid, and P. Doleschall, Phys. Rev. C **31**, 325 (1985).
[13] J. R. Taylor, Nuovo Cimento B **23**, 313 (1974); M. D. Semon and J. R. Taylor, Nuovo Cimento A **26**, 48 (1975).
[14] E. O. Alt, W. Sandhas, and H. Ziegelmann, Phys. Rev. C **17**, 1981 (1978); E. O. Alt and W. Sandhas, *ibid*. **21**, 1733 (1980).
[15] E. O. Alt, A. M. Mukhamedzhanov, M. M. Nishonov, and A. I. Sattarov, Phys. Rev. C **65**, 064613 (2002).
[16] E. O. Alt, P. Grassberger, and W. Sandhas, Nucl. Phys. **B2**, 167 (1967).
[17] N. W. Schellingerhout, L. P. Kok, S. A. Coon, and R. M. Adam, Phys. Rev. C **48**, 2714 (1993).
[18] I. J. Thompson, B. V. Danilin, V. D. Efros, J. S. Vaagen, J. M. Bang, and M. V. Zhukov, Phys. Rev. C **61**, 024318 (2000).
[19] R. Machleidt, Phys. Rev. C **63**, 024001 (2001).
[20] A. Deltuva, A. C. Fonseca, A. Kievsky, S. Rosati, P. U. Sauer, and M. Viviani, Phys. Rev. C **71**, 064003 (2005).